Multi-faceted particle pumps drive carbon sequestration in the ocean

Philip W. Boyd, Hervé Claustre, Marina Lévy, David Siegel, Thomas Weber

Multi-faceted particle pumps drive carbon sequestration in the ocean

Revised for Nature 10 January 2019

Philip W. Boyd[1] Hervé Claustre[2], Marina Levy[3], David A. Siegel[4], Thomas Weber[5]

[1]Institute for Marine and Antarctic Studies, University of Tasmania, Hobart, Tasmania, Australia

[2] Sorbonne Université & CNRS, Laboratoire d'Océanographie de Villefranche-sur-mer (LOV), 06230 Villefranche-sur-Mer, France.

[3]Sorbonne Université, LOCEAN-IPSL, CNRS/IRD/MNHN, 4 Place Jussieu, 75252 Paris CEDEX 05, France.

[4]Department of Geography & Earth Research Institute, University of California, Santa Barbara, Santa Barbara, CA, 93106, USA,

[5]Department of Earth and Environmental Sciences, University of Rochester, Rochester, NY 14627

Orchid #

Philip Boyd http://orcid.org/0000-0001-7850-1911

Hervé Claustre 0000-0001-6243-0258

Marina Levy 0000-0003-2961-608X

David Siegel https://orcid.org/0000-0003-1674-3055

Thomas Weber 0000-0002-4445-6742

The ocean's ability to sequester carbon out of contact with the atmosphere exerts an important control on global climate. The biological pump drives carbon storage in the deep ocean and is thought to function via gravitational settling of organic particles from surface waters. However, the settling flux alone is often insufficient to balance mesopelagic carbon budgets or meet the demands of subsurface biota. Here, we review additional biological and physical mechanisms that inject suspended and sinking particles to depth. Together, these "particle injection pumps" likely sequester as much carbon as the gravitational pump, closing carbon budgets and motivating further investigation of their environmental controls.

Introduction

Open ocean waters store (sequester) carbon out of contact with the atmosphere on decadal to millennial timescales, exerting a major control on global climate by regulating atmospheric carbon dioxide partial pressure (pCO_2)[1]. The magnitude of ocean carbon storage is governed by two well-established mechanisms that maintain a surface-to-deep ocean gradient of dissolved inorganic carbon (DIC) – the biological and the solubility pumps[2,3]. The solubility pump delivers cold, dense, DIC-rich waters to depth mostly at high latitudes, whereas the biological pump globally exports particulate organic carbon (POC) from surface waters. POC export is largely attributed to the gravitational settling of a subset of the particle assemblage[1,4] – a process we refer to as the "biological gravitational pump" (BGP).

The BGP is the key link between upper ocean photosynthetic carbon fixation, the sustenance of mid-water biota, and carbon storage in the oceans' interior[4,5], and is thought to account for ~90% of the vertical DIC gradient, while the solubility pump explains the remainder[1]. In the absence of the BGP, models predict atmospheric pCO_2 would be higher by nearly twofold[6]. Contemporary and paleoceanographic observations both reveal that carbon sequestration by the BGP is affected by environmental changes in light, temperature, stratification and nutrient availability[7,8], and can itself drive dramatic climate shifts such as glacial-interglacial cycles[8]. Future climate projections suggest that the functioning of the BGP will be altered by ocean global change[7,9], potentially feeding back on anthropogenic climate warming[10]. As a consequence, quantification of its functioning requires a reliable baseline of accurate measurements.

The underlying principles of the BGP are long established[11]: organic particles are continually produced and recycled in sunlit surface waters, and a small fraction of these settle into the

oceans' interior. The strength of the BGP is often quantified as the rate of particle "export" from the euphotic zone, the surface mixed layer, or across an arbitrary horizon at 100m[12]. As they sink, particles undergo myriad transformations, which lead to pronounced vertical attenuation of the particle flux that is often described as a power law relationship, referred to as the "Martin Curve"[13]. The efficiency of the BGP is defined here as the time that exported carbon is kept sequestered from the atmosphere within the ocean's interior. It is driven by the depth scale of flux attenuation and pathways of ocean circulation that carry remineralized carbon dioxide back to the surface[14]. Carbon is sequestered for timescales longer than a year by particles that penetrate the permanent pycnocline (beneath the wintertime mixed layer) and up to centuries by those that reach deep water masses (generally >1000m). Together, the strength and efficiency of the BGP determine the total quantity of carbon sequestered biologically in the ocean interior.

Recently, analyses of global and regional ocean carbon budgets have identified conspicuous imbalances (i.e., two to three-fold less storage) when BGP export fluxes are compared with those derived from geochemical tracers[15,16], highlighting the need to reassess the pathways that contribute to carbon storage. Furthermore, rates of site-specific particle export appear to be insufficient to meet the carbon demand of mid-water life (termed mesopelagic biota) by two-to three-fold[17-20], but in one study can be balanced using community respiration[18]. There is considerable debate over the reasons for these carbon deficits, ranging from biases inherent in observational technologies[17,21] to the potential role of other carbon (dissolved and/or particulate) delivery mechanisms to deep waters[16,22,23]. Traditionally, the biogeochemical functioning of the BGP has been evaluated from quasi one-dimensional (1D) observations of particle flux (Box 1), and extrapolated using Earth System Models (ESMs, parameterised with observations[24-26]) and/or remote-sensing observations[26]. This approach cannot capture

more complex mechanisms of carbon export that are highly variable in space and time (Box 1), potentially resulting in the reported carbon budget deficits.

Multiple lines of research have revealed the importance of additional export pathways, physically (e.g. subduction) and/or biologically (e.g. large mesopelagic migrators) -mediated, that inject particles to depth, termed here Particle Injection Pumps (PIPs)[23,27-30]. These mechanisms can potentially export all particle classes to depth, and thus challenge the conventional view of gravitational sinking as the dominant downward pathway for particles into the oceans' interior. The characteristics of PIPs fundamentally change our understanding of biological carbon sequestration: first, PIPs can animate particle transport spatially into three dimensions (3D), in contrast with the BGP where the vertical dimension is predominant (1D); second, global estimates of PIP carbon fluxes are significant relative to those for the BGP[27,28], and third, these mechanisms cannot be readily quantified using the traditional toolbox applied to investigate the BGP (Box 1). Overall, the PIPs will increase the strength of the biological pump beyond estimates based on gravitational flux alone, and can change its efficiency by altering the depth of carbon export.

The fate of exported carbon following its delivery to depth has also proven more complex and heterogeneous than previously recognized. Particle flux attenuation is now known to vary systematically in space[14,31,32] and time[33], suggesting the traditional empirical view[13] must be replaced by a mechanistic one that considers particle composition and architecture, microbial metabolism, and transformation processes[17].

Together, these developments stand to reshape our understanding of particle transport and remineralisation in the oceans' interior. Here, for open ocean systems we review: the mechanisms, rates, and depths of particle injection by each PIP; the potential for each mechanism to close observed deficits in ocean carbon budgets; and the corresponding

130 remineralisation depths of exported POC in the deep ocean. We finish by outlining future
131 research directions needed to synthesize these developments into a new mechanistic, four-
132 dimensional (4D) view of carbon export and sequestration. The review does not detail the
133 important role of dissolved organic carbon subduction[22,23], nor cover the dark microbial
134 carbon pump[34] or chemolithotrophy[35] which have been reviewed elsewhere (S-Table 1).
135
136 **Particle injection pump mechanisms**
137 PIPs differ in their mechanisms, temporal-spatial scales (Fig. 1, Fig. 2a), and/or geographical
138 extent, but have common features: i) they can act on all particles from suspended to sinking
139 (Fig. 1); ii) they typically inject particles below the euphotic zone (i.e., the export depth for
140 the BGP), potentially reaching depths >1000m[28-30] depending on the injection mechanism
141 (Fig. 1, Fig. 2b); iii) they occur concurrently with the BGP but cannot be measured with
142 techniques developed to quantify gravitational settling[13,32] (Box 1); iv) their dynamic nature
143 (i.e., physical transport[23,27,28] or patchiness of animal distributions[30]) means that the interplay
144 between their vertical and horizontal vectors and temporal scales varies significantly (Fig. 1).
145 Hence, a 4D sampling framework is required to constrain them (Box 1). The main
146 characteristics of each PIP are elucidated below.
147 Particle export driven by physical subduction includes several processes driving the vertical
148 transport of near-surface particles that act on different space/time scales: subduction caused
149 by mixed-layer shallowing (termed the mixed-layer pump[29,36]); subduction by large-scale
150 (100-1000 km) circulation (termed the large-scale subduction pump)[23]; and subduction by
151 mesoscale (10-100 km) to submesoscale (1-10 km) frontal circulation (termed the eddy-
152 subduction pump[23,27,28]).

153 Carbon export by the mixed-layer pump is driven by biological accumulation of particles
154 throughout the spring/summer growth season, which are then diluted to the depth of the
155 mixed layer during winter, and left in the oceans' interior during early spring stratification
156 (Box 1). This pump operates on wide-ranging time-scales from days/weeks[37] to seasons[29,37],
157 predominantly in mid and high latitude regions characterised by strong seasonal variability in
158 mixed-layer depth (Fig. 2a). Although these concepts are long-established[36], only recently
159 have they been scrutinised in detail using advances in optical profiling (BGC-Argo) floats
160 and satellite particle proxies to track particle accumulation rates in relation to changes in
161 surface mixed-layer depth (Box 1).

162 The large-scale subduction pump is a 3D advective mechanism directed from the seasonal
163 mixed-layer into the oceans' interior, driven by Ekman pumping and horizontal circulation
164 across a sloping mixed-layer[38]. Subduction rates were first estimated for the North Atlantic[39],
165 and then globally using data-assimilating models[40]. The wide-ranging subduction rates (1-100
166 m/year)[39,40] are small relative to BGP particle settling rates[11,12], but subduction occurs over
167 large regions of the global ocean boosting the magnitude of carbon delivery to depth.

168 The frontal-associated eddy-subduction pump subducts particle-rich surface waters on
169 timescales of days and across spatial scales of 1-10 km, driven by strong vertical circulation
170 associated with fronts and eddies[27,28,41-44]. Gliders are now used to map 3D dynamic eddying
171 flow fields (Box 1), finding evidence for penetration of high particle stocks (co-located POC
172 and chlorophyll indicative of viable phytoplankton) from the spring bloom, conspicuous as
173 distinct filaments at 100-350 m depth at the eddy periphery[28] (Box 1). Mapping revealed the
174 co-location of high POC filaments and negative vorticity to depths near the permanent
175 pycnocline[28], and the mechanism is supported by high-resolution simulations in which eddy
176 subduction of particles is a recurring feature[45-48]. The strength of the eddy-subduction pump

177 is governed by the vigour and penetration of the vertical circulation, in conjunction with local
178 POC stocks over the frontal area[27,49]. Eddy subduction rates span 1-100 m d^{-1} (c.f. 20 to >
179 100 m d^{-1} for the BGP[11,12]) depending on the eddy or frontal structure. Modelling indicates
180 that these subducted particles are remineralised more rapidly (i.e., at relatively shallow depths)
181 relative to gravitationally-sinking particles[27].

182 The concept for the 'mesopelagic migrant pump' is based on long-established observations of
183 diurnal vertical migration[50] (Box 1). This pump extends the remineralisation scale by
184 injecting particles to greater depth before decomposition begins[51,52], as determined by gut
185 retention time of migrating animals[51-53] and the depth of their migration (typically ~400 m[53]).
186 The injected particles are zooplankton faecal pellets with sinking rates of 10-100's m d^{-1} (ref.
187 51), faster than loosely-packed organic aggregates settling from the surface[11,12], and will
188 penetrate deeper in the water column before remineralisation. This pump therefore influences
189 all important facets of the particle flux that govern carbon sequestration – total export rate,
190 depth of peak flux, and flux attenuation depth scale.

191 Diurnal vertical migration results in active subsurface transport and carbon sequestration, and
192 is usually reported for mesozooplankton and often included in BGP estimates[51]. However,
193 vertical migration by larger mesopelagic carnivorous organisms (from greater daytime depths
194 than mesozooplankton) are not sampled by conventional BGP approaches[52,54]. Targeted
195 studies (Box 1) have quantified this pump driven by large mesopelagic migrant carnivores in
196 the Pacific[54], and other regions (S-Table 1). The underlying mechanism is upward migration
197 to graze mesozooplankton[54] followed by rapid (hours) downward migration[53], with
198 respiration (release of CO_2), exudation, and defecation (release of POC/DOC)[51,55] often
199 below the permanent pycnocline[56], at depths up to 600m (Box 1).

Trawl surveys suggest that ~50% of mesopelagic organisms migrate, ranging regionally between 20-90% depending on temperature, turbidity and oxygen concentrations[54,56]. The carbon sequestration rate by this pathway is governed by the metabolic transfer efficiency of migrators, and particles are injected at their residence depth, often at the upper boundary of oxygen minimum zones where their respiration intensifies oxygen depletion[53].

Active transport by vertically-migrating metazoans can also occur on longer timescales (Box 1). For example, in high latitude regions the winter hibernation of copepods (members of the mesozooplankton) at depths between 600-1400m gives rise to a so-called 'seasonal lipid pump[30']: during hibernation, they catabolise carbon-rich lipids accumulated during summer in upper layers and thereby shunt carbon (but not nitrogen and phosphorus) below the permanent pycnocline[30]. The strength of the seasonal lipid pump is governed by copepod abundance, size and temperature, which together control their respiration rate and help explain the existence of carbon flux hotspots (i.e. patchiness)[30].

Another vertical export mechanism that operates on seasonal migration timescales is mortality at depth of hibernating zooplankton particularly in high latitude regions[57,58], sequestering carbon to depths >500 m depth. Global extrapolation of seasonal lipid pump fluxes, along with the over-wintering mortality flux is problematic due to difficulties in sampling and generalizing across distinct regional mechanisms[30] (S-Table 1).

The potential for double accounting

The export flux from the BGP is mediated by sinking particles, whereas PIPs can provide additional pathways for all particle classes, from suspended to sinking, to exit the surface ocean (Fig. 1). Thus, there is potential overlap between particles delivered from the surface ocean to depth via the BGP and by injection from PIPs. Such overlap – termed here as

224 'double-accounting' – may occur where particles associated with the BGP and a PIP are
225 difficult to distinguish and hence could be attributed to more than one pump (Fig. 1). At
226 depth, transformations such as aggregation alter particle characteristics, including size and
227 sinking rate, and hence particles injected by the PIPs can join the sinking flux usually
228 attributed the BGP (Fig. 1). A further factor that introduces overlap between the BGP and
229 PIPs results from the inclusion, for historical reasons[59], of one component of the mesopelagic
230 migration pump (diurnal migration by mesozooplankton) into the 1D sampling framework of
231 the BGP, while other components (e.g. patchier diurnal migration by larger mesopelagic
232 carnivores[5]) are not. Hence double-accounting can confound our understanding of the
233 relative importance of PIPs to ocean carbon storage.

234 Is it possible to tease apart these areas of overlap? Forty years study of the BGP has
235 uncovered a complex biogeochemical system with multiple drivers and distinguishing
236 characteristics[11,60]. This body of research helps to frame the differences and similarities
237 between particles delivered to depth by PIP's and those settling via the BGP. Each PIP is
238 distinct with respect to its combination of injected particle type (suspended cells to faecal
239 pellets of large mesopelagic migrants), the timing and depth of injection (Fig. 2a-b), and
240 associated particle transformations (aggregation/disaggregation)[11,12,61]. Additionally, the
241 subsurface "fate" of particles (i.e. where they remineralize), which determines the longevity
242 of carbon sequestration, is driven by the complex interplay between these properties and
243 transformations[12,60,61]: Particle composition and architecture set their sinking speed, while
244 myriad processes that are biologically- (microbes/zooplankton) and physically-mediated
245 (fragmentation/ disaggregation)[12,62-64] decompose and repackage them over depth (Fig. 1).
246 Therefore, particle fate provides another avenue to distinguish the contributions of PIPs from
247 the BGP.

To date, evidence on the subsurface fate of injected particles has been largely indirect[27,28,49]. Surveys of eddy-subduction pumps suggest that injected particles may be remineralised at depths <200 m, based on ammonium peaks[49], time-series of biogeochemical gradients[28], or particle modelling studies[27]. In the NE Atlantic, reported high rates of particle remineralisation (glider-based biogeochemical gradients) must be reconciled with concurrent evidence of coincident, coherent chlorophyll plumes at depths >300 m indicative of subducted viable phytoplankton[28]. This glider-based time-series reveals pronounced patchiness[28] suggesting that inference of the fate of injected particles even from state-of-the-art observations is challenging.

Better constraining the contribution of each PIP to mesopelagic carbon budgets will require characterisation of the injected particle assemblage and their transformations during downwards transport[12,65-68]. Particle aggregation in PIPs may be driven by convergence/subduction[69-70] and/or differential sinking[65,67], potentially leading to altered modes of subsurface transport (Fig. 1). BGC-Argo profile observations allow quantification of the size, type, seasonal succession, and penetration depths of particles injected by the mixed-layer pump[36] – properties which have the potential to differentiate them from fast-sinking particles (i.e., BGP) whose distinctive 'spiky' bio-optical signature is readily detected using multiple sensors[71] (S-Figs. 2 and 3). Advances in bio-optics are already making cryptic signatures associated with slow-sinking particles and zooplankton vertical migration less opaque, lessening the possibility of double-accounting. Such double-accounting may be avoided through the identification of unique characteristics of pumps including seasonality (Fig. 2a), distinctive regional features[30], or multi-variate oceanographic diagnostics[72].

Carbon sequestration potential

The potential carbon sequestration by each PIP can be quantified as the product of their carbon injection rate and their sequestration timescale, i.e. time until remineralised carbon is returned to the surface (see Supplementary Methods). This timescale is determined both by the injection depth of particles and their eventual fate, i.e. the degree to which they sink or circulate through the ocean before remineralising to CO_2. In general, deeper particle injection and rapid sinking translates to longer carbon sequestration because the "passage time" from the ocean interior to the surface increases with depth (Fig. 2b). Here, we assemble prior estimates of carbon injection rate and depth (S-Table 1), along with new modelling projections (Fig. 2), to estimate carbon sequestration by each PIP and assess their significance relative to the BGP.

Some targeted studies provide concurrent estimates of carbon injection by individual PIPs and the BGP[27,28], whereas others[30,54,57,58] facilitate comparison of regional-scale PIP fluxes with independent estimates of the BGP. Both approaches reveal that PIPs each have the potential to contribute significant rates of POC export. The reported upper bounds of global PIP estimates summed together is 8.7 Pg C yr^{-1}, which is comparable to the BGP export flux (Table S1). This comprises 1.1-2.1 Pg C yr^{-1} for the large-scale/mesoscale physical pumps (also includes DOC[22,23]), and 0.25-1.0, 0.9-3.6 and (-0.09) to 2.0 Pg C yr^{-1} from the lipid seasonal, mesopelagic migration, and eddy-subduction pumps, respectively (Fig. 2c). Thus, their cumulative contribution may be as much as ~40% of total particle export (i.e., BGP+PIPs) suggesting considerable potential to resolve the imbalances reported for mesopelagic carbon demand[17], between nutrient and carbon export budgets[15], and to lessen the variability between model estimates of global carbon sequestration (S-Table 1).

We estimated the sequestration timescales for each PIP based on the "passage time" from the injection depth to the surface in an observationally-constrained ocean circulation model[14]. Particles injected at the depth of the wintertime mixed-layer by the large-scale physical pumps (mixed-layer and subduction) result in sequestration for 25-100 years, assuming subduction occurs before re-entrainment next winter. In turn, deeper injection by the eddy subduction pump (up to 450 m), mesopelagic migration pump (up to 600 m), and seasonal lipid pump (up to 1400 m) translates to sequestration timescales up to 150, 250, and 500 years respectively (Fig. 2b). These timescales will increase if it is assumed that sinking rather than suspended particles are injected, which remineralise deeper than the injection horizon (see Supplementary Methods).

Given the wide-ranging estimates of carbon injection rate (Fig. 2c) and depth (Fig. 2b) for each PIP, oceanic carbon sequestration by these mechanisms cannot be estimated with precision (Fig. 2d). However, choosing central values from the reported ranges of each property allows a first order comparison between PIPs and the BGP. The mesopelagic migration pump emerges as the most significant PIP, potentially storing ~60% as much carbon as the BGP in the ocean interior if large, sinking particles (i.e. faecal pellets) are injected. The C storage potential of the seasonal lipid, eddy-subduction and large subduction pumps are ~20%, 10% and 5% of the BGP respectively, assuming each injects suspended particles. The latter small net value is due to offsetting of subduction by strong obduction (upward transport of water parcels) in the equatorial oceans[39]. Based on these central values (Fig. 2d), it is likely that the reservoir of respired carbon in the ocean interior contributed by the PIPs approaches that contributed by the BGP, and may therefore help to close global-scale mesopelagic carbon budgets[15,16].

Tracer constraints on the fate of exported carbon

Oceanic carbon sequestration by the BGP and wide-ranging biophysical mechanisms that inject biogenic particles to depth depends critically on the fate of exported carbon (Fig. 2). However, at present tracing the remineralisation of particles (regardless of their export pathway) as they settle and circulate through the global ocean remains a logistical challenge, due to the difficulties of deep-water particle sampling. Recently, new methods have used 3D ocean data assimilation models to leverage geochemical "remineralisation tracers" including oxygen and nutrients. These tracers integrate particle remineralisation signatures over long timescales, and their global distributions are characterised by orders of magnitude more observations than are available for particles[16,31,73]. Two distinct approaches have been applied. The first diagnoses remineralisation rates directly from phosphate accumulation along transport pathways in a circulation model, and reconstructs particulate flux profiles required to explain the global distribution of remineralised phosphate[31]. The second assimilates geochemical and satellite data into mechanistic biogeochemical models to optimise key particle flux parameters, yielding mechanistic insights while leveraging the observations less directly[73].

Both approaches have yielded similar results and provide evidence for regional variability in particle flux attenuation, with the flux attenuating slowly at high latitudes and quickly in subtropical gyres, while the tropics lie between these two extremes (Fig. 3a). These simulations reveal that carbon exported from high latitude and tropical surface waters is sequestered longer in the oceans' interior than carbon exported in the oligotrophic gyres (Figure 3b), with important implications for feedbacks between the particle export and global climate. Atmospheric pCO_2 is likely more sensitive to past changes in high latitude export than previously recognised[8], and the future expansion of subtropical habitats[9] may result in less efficient (although not currently quantifiable) carbon sequestration in a warming world.

Regional variations in particle flux attenuation have largely been interpreted in terms of the balance between decomposition and sinking rates[32]. A likely explanation for the diagnosed latitudinal pattern is the temperature-dependent metabolism of heterotrophs responsible for particle decomposition[32,73], although variations in particle size and/or ballast are valid alternatives[73]. There may also be a secondary effect of oxygen, with decomposition slowing in anoxic zones[73,74], and even hypoxic waters due to anaerobic microenvironment formation in particles[75].

To some degree, model-derived particle flux profiles may also reflect the relative magnitude of different export pathways (PIPs and BGP), which vary in the injection depth and nature of particles they supply, since geochemical tracers integrate the effects of all export mechanisms. Deep injection by PIPs would result in slower flux attenuation over depth, whereas injection of suspended particles that remineralise shallower in the water column would be diagnosed as rapid flux attenuation. Predicting future changes in ocean carbon sequestration will require a better understanding of the contribution of injection versus remineralisation processes to sequestration efficiency (Fig. 3b), given the different environmental sensitivity of these processes.

The need for prediction motivates development of new techniques to distinguish particle flux associated with the BGP and each PIP. Particle stoichiometry (i.e., C:N:P) may be central to identifying particular mechanisms that decouple their export. For example, diagnosing oxygen consumption between 500-1500 m (depth of zooplankton hibernation) without concomitant nutrient accumulation would point to carbon export by the seasonal lipid pump[30]. Alternatively, diagnosing seasonal cycles of nutrient accumulation and oxygen consumption rates would help distinguish remineralisation of particles exported by physical pumps versus particle settling, which should exhibit distinct seasonality (Fig. 2a). This approach may soon

be possible given the burgeoning spatial/temporal resolution of tracer data provided by BGC-Argo floats (S-Figure 1), and emerging float sensor technology (S-Table 2).

Extrapolation – towards a 4D view of particle export

Improving the accuracy of the initial estimates of the magnitude of carbon sequestration presented in Figure 2d requires the development of a 4D picture of particle flux and storage in the oceans' interior. It is clear from our synthesis of PIP mechanisms that multiple scales, from sub-mesoscale to basin, must be accommodated if PIPs are to be assembled, first spatially and then temporally, into a complete 4D picture. Again, lessons on how to approach such upscaling can be gleaned from BGP research which imprinted both spatial and seasonal signatures (satellite remote-sensing/modelling)[26] onto short-term (days-weeks) observations taken at specific sites (Box 1). The timescales and lifetimes of features such as submesoscale eddies/fronts or seasonal mesopelagic export signatures (Fig. 2a) must be characterized to define the temporal footprint of each PIP and move towards a 4D viewpoint. This framework must be linked to the seasonality of pelagic particle production to assess if there is distinctive period for the subduction of significant stocks of these upper ocean particles (Fig. 2a). For example, it is well-established that submesoscale dynamics are strongly seasonal, with stronger and deeper penetration during winter than summer[76].

Some published approaches towards extrapolating PIP's globally, and to climatological time scales, are outlined in S-Table 1. The identification of the specific drivers of each PIP mechanism should help improve modelling and hence extrapolation. We advocate the utility of explicitly incorporating the different PIP mechanisms into predictive, mechanistic models as a means to extrapolate PIPs into 4D. In the case of the extrapolation of the submesoscale eddy subduction PIP, increasing the model grid resolution to incorporate these features is

392 necessary and is now achievable in regional configurations[77,78]. In contrast, other physically-
393 mediated PIPs such as the large-scale subduction and mixed-layer pumps are already
394 represented in global models, and so their extrapolation requires the development of
395 diagnostics to enable the simulated POC/DOC distributions to be better evaluated against
396 observations[23]. At present, the biologically-mediated PIPs are not incorporated into state-of-
397 the-art biogeochemical models[9,14,31,77,78]. While simulating animal behaviour at the global
398 scale remains a grand challenge in ocean modelling, simple parameterisations have been
399 developed to predict the geochemical effect of the mesopelagic migrant pump[6], which might
400 be further expanded to incorporate hibernation and therefore the seasonal lipid pump. It is
401 only very recently that diel vertical migration has been incorporated for the first time in a
402 global ocean general circulation model and used to estimate the associated flux of carbon at
403 the global scale (see Aumont et al. in S-Table 1). Although promising, this approach remains
404 challenging because it is based on a computationally-intensive, end-to-end ecosystem model
405 in which all trophic levels from phytoplankton to top predators interact.

406

407 **Transforming our view of ocean carbon export**

408 Our synthesis of physically- and biologically-mediated PIPs reveals that they are directly
409 transporting significant stocks of biogenic particles to depth, of a cumulative magnitude that
410 may be equivalent to the carbon storage of the BGP. The potential of PIPs to make a major
411 contribution to the ocean carbon budget must now be explored in more detail, commencing
412 with those PIPs that are most likely to contribute to carbon sequestration. Synthesising
413 estimates of particle export, injection depth, and circulation timescales reveals that the
414 mesopelagic migrant pump has the greatest potential to contribute to carbon sequestration,
415 followed by the seasonal lipid pump and the various physical pumps (Fig. 2d). In the case of

416 the seasonal lipid pump, its geographical realm of influence is already established[30], whereas
417 less is known about the regional contributions of the mesopelagic migrant pump[5].

418 For all PIPs, the most pressing research issue – needed to address double-accounting issues
419 and improve estimates of carbon sequestration – is to better understand the mechanisms of
420 particle transformations[17,65-68] (Fig. 1) within a 4D framework. Specifically, the fate of
421 exported particles between their injection depth and the permanent pycnocline remains poorly
422 constrained. A first step will be improved particle characterisation, in particular the ability to
423 distinguish zooplankton from other particle types, and to aggregate Particle Size Distribution
424 (PSD) profiles through the development and application of new sensors (S-Table 2). Future
425 development of acoustic and imaging technologies[79] must be deployed on a range of
426 platforms from ships (i.e., calibration) to an array of long-lived (i.e., years), geographically-
427 diverse BGC-Argo floats. These developments towards improving particle characterisation
428 will reduce the likelihood of double-accounting. Moreover, the alignment of BGC-Argo
429 deployments (Box 1) with the characteristic space and time scales of PIPs will enable better
430 quantification of the role of patchiness in driving observed local/regional hotspots in
431 biological PIPs[30,54,56]. In time, following the development and testing of a Coastal-Argo
432 platform, they can also be deployed to coastal and shelf seas to explore the role of PIPs in
433 these regions (S-Table 2).

434 The way forward in refining estimates of the contribution of PIPs in closing the ocean carbon
435 budget[15-17] also requires leveraging advancements in ocean biogeochemical modelling.
436 Models are valuable testbeds to probe the sensitivity of carbon storage mechanisms, and
437 guide future observations. For example, model sensitivity analyses point to the pivotal role
438 of PSD in determining the fate of exported carbon[31,73], but the processes that set the PSD of
439 exported particles and its evolution over depth remain crudely parameterized. Developing
440 robust models of particle transformations between multiple size classes, and incorporating

441 them into general circulation models, will allow us to trace the fate of particles injected by
442 different PIPS and dissect their contribution to carbon sequestration, while avoiding double-
443 accounting issues.

444 Inverse methods that can assimilate PSD fields from new BGC-Argo technologies[80] will
445 allow models to "learn" from the data, further refining them to best reflect the real ocean.
446 Furthermore, downscaling of physical models is essential to simulate the locations of PIP
447 injections in support of observational programmes such as high resolution altimetry[81], and the
448 integration of detailed particle transformations into submesoscale models[82].

449 To transform the comprehension of particle export from one- to three- and eventually four-
450 dimensions, machine learning approaches[83] will need to be employed, which can be trained to
451 predict unknown variables such as particle flux from better sampled variables. Approaches
452 like artificial neural networks[84], will enable and enhance the upscaling of local/regional
453 datasets needed to provide more robust extrapolation[85,86] to depth, regionally, and annually of
454 each PIP. This upscaling is essential to refine estimates of the contribution of each PIP to
455 carbon sequestration. BGC-Argo datasets will also eventually be combined with new satellite
456 products such as hyperspectrally-resolved ocean colour observations of biology processes[87]
457 and submesoscale characterisation of sea level using high-resolution altimetry[81].

458 Satellite and water-column remote-sensing, along with targeted process studies, will yield
459 expansive datasets that can be assimilated into regional and global models of ever increasing
460 realism and resolution. Together, these approaches will lead towards a robust, four-
461 dimensional view of carbon sequestration by the ocean's multi-faceted bio-physical particle
462 pumps.

463

464

Acknowledgements

The authors thank five anonymous reviewers for improving the manuscript. PWB was primarily supported by the Australian Research Council through a Laureate (FL160100131), and this research was also supported under Australian Research Council's Special Research Initiative for Antarctic Gateway Partnership (Project ID SR140300001). HC acknowledges the support of the European Research Council (remOcean project, grant agreement 246777) and of the Climate Initiative of the BNP Paribas foundation (SOCLIM project). ML was supported by CNES and by the ANR project SOBUMS (ANR-16-CE01-0014). DAS acknowledges support from the National Aeronautics and Space Administration as part of the EXport Processes in the global Ocean from RemoTe Sensing (EXPORTS) field campaign - grant 80NSSC17K0692. TW was supported by NSF grant OCE-1635414. Co-authors, HC, ML, DS and TW contributed equally to this Review.

499 References

500 1Sarmiento, J. L. & Gruber, N. (2006). Ocean Biogeochemical Dynamics. (Princeton
501 University Press, 2006).

502 2Volk, T., and M. Hoffert (1985). Ocean carbon pumps: Analysis of relative strengths and
503 efficiencies in ocean-driven atmospheric CO_2 changes, in The Carbon Cycle and
504 Atmospheric CO_2: Natural Variations Archean to Present, Geophys. Monogr. Ser., vol. 32,
505 edited by E. T. Sundquist and W. S. Broecker, pp. 99–110, AGU, Washington, D. C.

506 3McKinley GA, Pilcher DJ, Fay AR, Lindsay K, Long MC, Lovenduski NS. (2016).
507 Timescales for detection of trends in the ocean carbon sink. Nature 530:469–72

508 4Buesseler, K. O., Lamborg, C. H., Boyd, P. W., Lam, P. J., Trull, T. W., and co-authors
509 (2007). Revisiting carbon flux through the ocean's twilight zone through the ocean's twilight
510 zone. Science, 316, 567-570. doi: 10.1126/science.1137959.

511 5Irigoien, X. et al. (2014). Large mesopelagic fishes biomass and trophic efficiency in the
512 open ocean. Nat. Commun. 5, ncomms4271.

513 6Maier-Reimer E., U. Mikolajewicz, A. Winguth (1996). Future ocean uptake of CO_2:
514 interaction between ocean circulation and biology. Climate Dynamics, 12, 711-721.

515 7Bopp, L., et al. (2013), Multiple stressors of ocean ecosystems in the 21st century:
516 Projections with CMIP5 models, Biogeosciences, 10, 6225–6245.

517 8Martinez-Garcia, A. et al. (2014). Iron fertilization of the Subantarctic Ocean during the last
518 ice age. Science 343, 1347–1350.

519 9Moore J.K. et al. (2018) Sustained climate warming drives declining marine biological
520 productivity. Science, 2018; 359 (6380): 1139 DOI: 10.1126/science.aao6379

521 10Bernardello R. et al. (2015) Response of the ocean natural carbon storage to projected
522 twenty-first-century climate change J of Climate DOI: 10.1175/JCLI-D-13-00343.1

523 11Boyd, P. W. & Trull, T. W. (2007). Understanding the export of biogenic particles in
524 oceanic waters: Is there consensus? Progress in Oceanography, 72(4), 276-312. doi:
525 10.1016/j.pocean.2006.10.007

526 12Buesseler, K.O., and Boyd, P.W. (2009). Shedding light on processes that control particle
527 export and flux attenuation in the twilight zone of the open ocean. Limnol. Oceanogr. 54,
528 1210–1232.doi:10.4319/lo.2009.54.4.1210

529 13Martin, J., G. Knauer, D. Karl, and W. Broenkow (1987), VERTEX: Carbon cycling in the
530 northeast Pacific, Deep Sea Res., Part A, 34, 267–285.

531 14DeVries, T., F. Primeau, and C. Deutsch (2012). The sequestration efficiency of the
532 biological pump, Geophysical Research Letters, 39, doi:10.1029/2012GL051963.

533 15Emerson, S. (2014) Annual net community production and the biological carbon flux in the
534 ocean. Global Biogeochemical Cycles 28, 1–12, doi:10.1002/2013GB004680

16Schlitzer, R. (2002) Carbon export fluxes in the Southern Ocean: results from inverse modeling and comparison with satellite based estimates, Deep-Sea Research II, 49, 1623-1644.

17Burd, A. B. et al. (2010). Assessing the apparent imbalance between geochemical and biochemical indicators of meso- and bathypelagic biological activity: What the @$#! is wrong with present calculations of carbon budgets? Deep-Sea Res. Part II Top. Stud. Oceanogr. 57: 1557–1571. doi:10.1016/j.dsr2.2010.02.022

This paper reviewed the (lack of) progress on constraining mesopelagic carbon budgets, and advocated new approaches to tackle this issue.

18Giering, S. L. et al. (2014). Reconciliation of the carbon budget in the ocean's twilight zone. Nature 507, 480–483. doi: 10.1038/nature13123

This paper presented one of the few balanced mesopelagic carbon budgets by assessing community respiration versus carbon demand.

19Steinberg, D.K., B.A.S. Van Mooy, K.O. Buesseler, P. W. Boyd, T. Kobari, and D.M. Karl (2008). Bacterial vs. zooplankton control of sinking particle flux in the ocean's twilight zone. Limnol. Oceanogr. 53: 1327–1338.

20Reinthaler, T. et al. (2006). Prokaryotic respiration and production in the meso- and bathypelagic realm of the eastern and western North Atlantic basin. Limnol. Oceanogr. 51: 1262–1273.

21Boyd, P.W., McDonnell, A., Valdez, J. (2015) RESPIRE: An in situ particle interceptor to conduct particle remineralization and microbial dynamics studies in the oceans' Twilight Zone. Limnology and Oceanography-Methods Volume: 13s: 494-508.

22Hansell D.A., Carlson C.A., Repeta D.J., Schlitzer R., (2009). Dissolved organic matter in the ocean. Oceanography 22:52–61.

23Lévy, M., Bopp, L., Karleskind, P., Resplandy, L., Ethé, C., & Pinsard, F. (2013). Physical pathways for carbon transfers between the surface mixed layer and the ocean interior. Global Biogeochemical Cycles, 27(4), 1001–1012. http://doi.org/10.1002/gbc.20092.

24Henson, S. A., Yool, A., & Sanders, R. (2015). Variability in efficiency of particulate organic carbon export: A model study. Geophysical Res. Lett., 29, 33–45. http://doi.org/doi:10.1002/2014GB004965

25Aumont, O., Van Hulten, M., Roy-Barman, M., Dutay, J.-C., Ethé, C., & Gehlen, M. (2017). Variable reactivity of particulate organic matter in a global ocean biogeochemical model. Biogeosciences, 14(9), 2321–2341. http://doi.org/10.5194/bg-14-2321-201713

26Siegel, D. A., K. O. Buesseler, S. C. Doney, S. F. Sailley, M. J. Behrenfeld, and P. W. Boyd (2014), Global assessment of ocean carbon export by combining satellite observations and food-web models, Global Biogeochem. Cycles, 28, 181–196, doi:10.1002/2013GB004743.

27Stukel M.R., H. Song, R. Goericke, A.J. Miller (2017) The role of subduction and gravitational sinking in particle export, carbon sequestration, and the remineralization length

scale in the California Current Ecosystem. Limnology and Oceanography, doi: 10.1002/lno.10636

28Omand, M.M. et al. (2015). Eddy-driven subduction exports particulate organic carbon from the spring bloom. Science 348,222–225.doi:10.1126/science.1260062.

This paper quantified the Eddy Subduction Pump (ESP) using an array of gliders in the North Atlantic during the spring bloom.

29Dall'Olmo G., J. Dingle, L. Polimene, R.J.W. Brewin and H.Claustre (2016). Substantial energy input to the mesopelagic ecosystem from the seasonal mixed-layer pump. Nature Geoscience, 9, 820-825 DOI: 10.1038/NGEO2818.

This paper quantified the Mixed Layer Pump (MLP) across large regions of the high latitude ocean.

30 Jónasdóttir S.H, Richardson K., Heath M.R. 2015. Seasonal copepod lipid pump promotes carbon sequestration in the deep North Atlantic. PNAS 112:12122–26.

This paper provided the first detailed quantification of the seasonal lipid pump (SLP).

31Weber T. et al. (2016), Deep ocean nutrients imply large latitudinal variation in particle transfer efficiency. PNAS, 113, 8606–8611.

32Marsay, C. M., R. J. Sanders, S. A. Henson, K. Pabortsava, E. P. Achterberg, and R. S. Lampitt (2015), Attenuation of sinking particulate organic carbon flux through the mesopelagic ocean, Proc. Natl. Acad. Sci. U.S.A, 112, 1089–1094.

32Giering, S. L. C., R. Sanders, A. P. Martin, S. A. Henson, J. S. Riley, C. M. Marsay, and D. G. Johns (2017), Particle flux in the oceans: Challenging the steady state assumption, Global Biogeochem. Cycles, 31, 159–171, doi: 10.1002/2016GB005424.

34Jiao N., et al. 2010. Microbial production of recalcitrant dissolved organic matter: long-term carbon storage in the global ocean. Nat. Rev. Microbiol. 8:593–599.

35Swan, B.K. et al. (2011) Potential for Chemolithoautotrophy Among Ubiquitous Bacteria Lineages in the Dark Ocean. Science, 333, 1296-1300.

36Bishop, J. K. B., M. H. Conte, P. H. Wiebe, M. R. Roman, and C. Langdon (1986), Particulate matter production and consumption in deep mixed layers: Observations in a warm-core ring, Deep Sea Res. Part A, 33, 1813–1841.

37Dall'Olmo, G., and K. A. Mork (2014), Carbon export by small particles in the Norwegian Sea, Geophys. Res. Lett., 41, 2921–2927, doi:10.1002/2014GL059244.

38Cushman-Roisin, B. (1987). Subduction. Hawaii Univ, Dynamics of the Oceanic Surface Mixed Layer P 181-196.

39Marshall, J., Nurser, A. & Williams, R. Inferring the subduction rate and period over the North Atlantic. J. Phys. Oceanogr. 23, 1315–1329 (1993).

40Liu, L. L., Huang, R. X., 2012. (2012). The global subduction/obduction rates: Their interannual and decadal variability. Journal of Climate, 25(4), 1096–1115. http://doi.org/10.1175/2011JCLI4228.1

41Pollard R. T. & L. Regier (1990) Large variations in potential vorticity at small spatial scales in the upper ocean. Nature 348, 227–229 doi:10.1038/348227a0.

42Nurser, A., & Zhang, J. (2000). Eddy-induced mixed layer shallowing and mixed layer/thermocline exchange. Journal of Geophysical Research Ocean, 105(C9), 21851.

43Niewiadomska, K., Claustre, H., Prieur, L., & D'Ortenzio, F. (2008). Submesoscale physical-biogeochemical coupling across the Ligurian Current (northwestern Mediterranean) using a bio-optical glider. Limnol. Oceanogr, 53, 2210–2225.

44Estapa, M. L., D. A. Siegel, K. O. Buesseler, R. H. R. Stanley, M. W. Lomas, and N. B. Nelson (2015), Decoupling of net community and export production on submesoscales in the Sargasso Sea, Global Biogeochem. Cycles, 29, 1266–1282, doi:10.1002/2014GB004913

45Lévy, M, Klein, P. and A.-M. Treguer (2001). Impacts of sub-mesoscale physics on phytoplankton production and subduction, J. Mar. Res., 59,535-565 doi: 10.1357/002224001762842181

46Nagai, T., Gruber, N., Frenzel, H., Lachkar, Z., McWilliams, J. C., & Plattner, G.-K. (2015). Dominant role of eddies and filaments in the offshore transport of carbon and nutrients in the California Current System. J. Geophys. Res. Ocean, http://doi.org/10.1002/2015JC010889

47Karleskind, P., Lévy, M., & Memery, L. (2011). Modifications of mode water properties by sub-mesoscales in a bio-physical model of the Northeast Atlantic. Ocean Modelling, 39, 47–60.

48Karleskind, P., Lévy, M., & Memery, L. (2011). Subduction of carbon, nitrogen, and oxygen in the northeast Atlantic. Journal of Geophysical Research Ocean, 116(C2), C02025. http://doi.org/10.1029/2010JC006446

49Stukel, M. R. et al. (2017). Mesoscale ocean fronts enhance carbon export due to gravitational sinking and subduction. Proc. Natl. Acad. Sci. USA. 114: 1252–1257. doi:10.1073/pnas.1609435114

This paper compared the magnitude of export fluxes from the biological pump and the Eddy Subduction Pump (ESP).

50Vinogradov M.E. (1997) Some Problems of Vertical Distribution of Meso- and Macroplankton in the Ocean. Advances in Marine Biology Volume 32, 1997, Pages 1-92. https://doi.org/10.1016/S0065-2881(08)60015-2

51Steinberg D.K., and M.R. Landry (2017). Zooplankton and the ocean carbon cycle. Annu. Rev. Mar. Sci. 2017. 9:413–44

52Bianchi D., Stock C., Galbraith E.D., Sarmiento J.L. (2013). Diel vertical migration: ecological controls and impacts on the biological pump in a one-dimensional ocean model. Glob. Biogeochem. Cycles 27:487–91

53Bianchi, D., Galbraith, E. D., Carozza, D. A., Mislan, K. A. S., & Stock, C. A. (2013). Intensification of open-ocean oxygen depletion by vertically migrating animals. *Nature Geoscience*, *6*(7), 545.

This paper used global Acoustic Doppler Current Profiler observations to constrain the Mesopelagic Migration Pump.

54Davison, P.C., Checkley Jr., D.M., Koslow, J.A., Barlow, J., (2013). Carbon export mediated by mesopelagic fishes in the northeast Pacific Ocean. Progress in Oceanography 116, 14–30.

This paper used trawl surveys and metabolic modelling to assess the export fluxes mediated by mesopelagic fishes.

55Childress, J. J., S. M. Taylor., G. M. Cailliet and M. H. Price (1980) Patterns of growth, energy utilization and reproduction in some meso- and bathypelagic fishes off Southern California. Marine Biology 61, 27-40 (1980)

56Klevjer T. A., X. Irigoien, A. Røstad, E. Fraile-Nuez, V. M. Benítez-Barrios & S. Kaartvedt. (2016). Large scale patterns in vertical distribution and behaviour of mesopelagic scattering layers. Scientific Reports, 6:19873, DOI: 10.1038/srep19873

57Bradford-Grieve JM, Nodder SD, Jillett JB, Currie K, Lassey KR. (2001). Potential contribution that the copepod *Neocalanus tonsus* makes to downward carbon flux in the Southern Ocean. J. Plankton Res. 23: 963– 75

58Kobari T, Steinberg DK, Ueda A, Tsuda A, Silver MW, Kitamura M. (2008). Impacts of ontogenetically migrating copepods on downward carbon flux in the western subarctic Pacific Ocean. Deep-Sea Res. II, 55:1648–60.

59Dam, H.G., C.A. Miller and S.H. Jonasdottir (1993) The trophic role of mesozooplankton at 47N, 20W during the North Atlantic Bloom Experiment. Deep-Sea Res. II, 40, 197-212.

60Turner J.T. (2015). Zooplankton fecal pellets, marine snow, phytodetritus and the ocean's biological pump. Prog. Oceanogr. 130:205–48

61Bishop, J.K.B. (1989) Regional extremes in particulate matter composition and flux: effects on the chemistry of the ocean interior. W.H. Berger, V.S. Smetacek, G. Wefer (Eds.), Productivity of the ocean: present and past, Dahlem Konferenzen, John Wiley & Sons, New York (1989), pp. 117-137

62McDonnell, A. M. P., P. W. Boyd, K. O. Buesseler (2015) Effects of sinking velocities and microbial respiration rates on the attenuation of particulate carbon fluxes through the mesopelagic zone. Global Biogeochemical Cycles. DOI: 10.1002/2014GB004935.

63Durkin, C.A., M.L. Estapa, and K.O. Buesseler (2015) Observations of carbon export by small sinking particles in the upper mesopelagic. Marine Chemistry, 175, 72-81.

64Cavan EL, Trimmer M, Shelley F, Sanders R, (2017) Remineralization of particulate organic carbon in an ocean oxygen minimum zone, Nature Communications, 8 Article 14847. ISSN 2041-1723.

65Alldredge, A.L., Silver, M.W., (1988). Characteristics, dynamics and significance of marine snow. Progress in Oceanography 20, 41–82.

66Jackson, G.A. (1990) A model of the formation of marine algal flocs by physical coagulation processes. Deep Sea Research Part A. Oceanographic Research Papers 37 (8), 1197-1211, 1990.

67Kiørboe, T., (2001). Formation and fate of marine snow: small-scale processes with large-scale implications. Scientia Marina 65 (Suppl. 2), 57–71.

68Iversen, M.H., Ploug, H., (2013). Temperature effects on carbon-specific respiration rate and sinking velocity of diatom aggregates – potential implications for deep ocean export processes. Biogeosciences 10, 4073–4085.

69Ohman M.D., R. Powell, M. Picheral and D.W. Jensen (2010) Mesozooplankton and particulate matter responses to a deep-water frontal system in the southern California Current System J. Plankton Res. 34, 815–827.

70D'Asaro, E. A. et al. (2018). Ocean convergence and the dispersion of flotsam. Proceedings of the National Academy of Sciences, 30, 201718453–6. http://doi.org/10.1073/pnas.1718453115

71Briggs, N., M. J. Perry, I. Cetinic, C. Lee, E. D'Asaro, A. M. Gray, and E. Rehm (2011), High-resolution observations of aggregate flux during a sub-polar North Atlantic spring bloom, Deep Sea Res. Part I, 58(10), 1031–1039.

72Stanley R.H.R., D.J. McGillicuddy Jr. Z. O. Sandwith, H. M. Pleskow (2017) Submesoscale hotspots of productivity and respiration: Insights from high resolution oxygen and fluorescence sections. Deep-Sea Research I, https://doi.org/10.1016/j.dsr.2017.10.005

73DeVries, T., and T. Weber (2017), The export and fate of organic matter in the ocean: New constraints from combining satellite and oceanographic tracer observations, Global Biogeochem. Cycles, 31, 535–555, doi:10.1002/2016GB005551.

74Cram, J.A., T. Weber, S.W. Leung, A.M.P. McDonnell, J._H. Liang, C. Deutsch (2018), The role of particle size, ballast, temperature, and oxygen in the sinking flux to the deep sea. Glob. Biogeo. Cyc. https://doi.org/10.1029/2017GB005710.

75Bianchi D., T.S.Weber, R. Kiko, C. Deusch (2018). Global niche of marine anaerobic metabolisms expanded by particle microenvironments. NGEO in press. https://doi.org/10.1038/s41561-018-0081-0.

76Callies, J., Ferrari, R., Klymak, J. M., & Gula, J. (2015). Seasonality in submesoscale turbulence. Nature Communications, 6, 6862–9. http://doi.org/10.1038/ncomms7862

77 Lévy, M. et al. (2012). Large-scale impacts of submesoscale dynamics on phytoplankton: Local and remote effects, 43-44(C), 77–93. http://doi.org/10.1016/j.ocemod.2011.12.003.

78Harrison, C. S., Long, M. C., Lovenduski, N. S., & Moore, J. K. (2018). Mesoscale effects on carbon export: A global perspective. Global Biogeochemical Cycles, 32, 680–703. https://doi.org/10.1002/2017GB005751

79Picheral, M., L. Guidi, L. Stemmann, D.M. Karl, G. Iddaoud Ghizlaine and G. Gorsky (2010), The Underwater Vision Profiler 5: An advanced instrument for high spatial resolution

727 studies of particle size spectra and zooplankton, Limnol. Oceanogr. Methods, 8,
728 doi:10.4319/lom.2010.8.462.

729 80Johnson K. (2017). Biogeochemical sensors for autonomous, Lagrangian platforms:
730 Current status, future directions. Autonomous and Lagrangian Platforms and Sensors ALPS
731 II. https://alps-ocean.us/agenda/(last accessed 16 March 2017).

732 81Ubelmann, C. and L.-L. Fu, (2014) On the transition from profile altimeter to swath
733 altimeter for observing global ocean surface topography. J. Atmos. Oceanic Tech., 31, 560-
734 568.

735 82Resplandy, L. et al. (2012). How does dynamical spatial variability impact 234Th-derived
736 estimates of organic export? Deep Sea Res. I, 68(C), 24–45.
737 http://doi.org/10.1016/j.dsr.2012.05.015

738 83Castelvecchi, D. (2016). Can we open the black box of AI? Nature, 528, 20-23.
739 doi:10.1038/538020a.

740 84Sauzède, R. et al. (2016). A neural network-based method for merging ocean color and
741 Argo data to extend surface bio-optical properties to depth: Retrieval of the particulate
742 backscattering coefficient. Journal of Geophysical Research-Oceans, 121(4), 2552-2571.
743 doi:10.1002/2015jc011408.

744 85Landschützer, P., N. Gruber, D. C. E. Bakker, U. Schuster, S. Nakaoka, M. R. Payne, T.
745 Sasse, and J. Zeng (2013), A neural network-based estimate of the seasonal to inter-annual
746 variability of the Atlantic Ocean carbon sink, Biogeosciences, 10, 7793–7815,
747 doi:10.5194/bg-10-7793-2013.

748 86Landschützer, P., N. Gruber, D.C.E. Bakker, and U. Schuster (2014). Recent variability of
749 the global ocean carbon sink. Global Biogeochemical Cycles, 28(9), 927-949.
750 doi:10.1002/2014gb004853.

751 87Werdell, P.J., L. I. W. McKinna, E. Boss, S. G. Ackleson, S. E. Craig, W. W. Gregg, Z.
752 Lee, S. Maritorena, C. S. Roesler, C. S. Rousseaux, D. Stramski, J. M. Sullivan, M. S.
753 Twardowski, M. Tzortziou, and X. Zhang, (2018), An overview of approaches and challenges
754 for retrieving marine inherent optical properties from ocean color remote sensing. Prog.
755 Oceanogr. 160, 186–212.

756 88Boyd, P.W. et al. (2005). The evolution and termination of an iron-induced mesoscale
757 bloom in the northeast subarctic Pacific Ocean. Limnology and Oceanography 50, 1872–
758 1886.

759 89Ohman, M.D., J.-B. Romagnan (2016) Nonlinear effects of body size and optical
760 attenuation on Diel Vertical Migration by zooplankton. Limnol. Oceanogr. 61, 2016, 765–
761 770.

762 90Powell, J.R., and M.D. Ohman (2012) Use of glider-class acoustic Doppler profilers for
763 estimating zooplankton biomass J. Plankton. Res, 34, 563–568.

764 91Siegel, D. A., and W. G. Deuser. (1997). Trajectories of sinking particles in the Sargasso
765 Sea: Modeling of statistical funnels above deep-ocean sediment traps. Deep-Sea Res. Part I
766 Oceanogr. Res. Pap. 44: 1519–1541. doi:10.1016/S0967-0637(97)00028-9

92Siegel, D. A., E. Fields, and K. O. Buesseler (2008), A bottom-up view of the biological pump: Modeling source funnels above ocean sediment traps, Deep Sea Res. Part I, 55(1), 108–127, doi:10.1016/j.dsr.2007.10.006.

93Llort, J., Langlais, C., Matear, R., Moreau, S., Lenton, A., Strutton, P.G., (2018). Evaluating Southern Ocean carbon eddy-pump from biogeochemical Argo floats. Journal of Geophysical Research: Oceans. https://doi.org/10.1002/2017JC012861

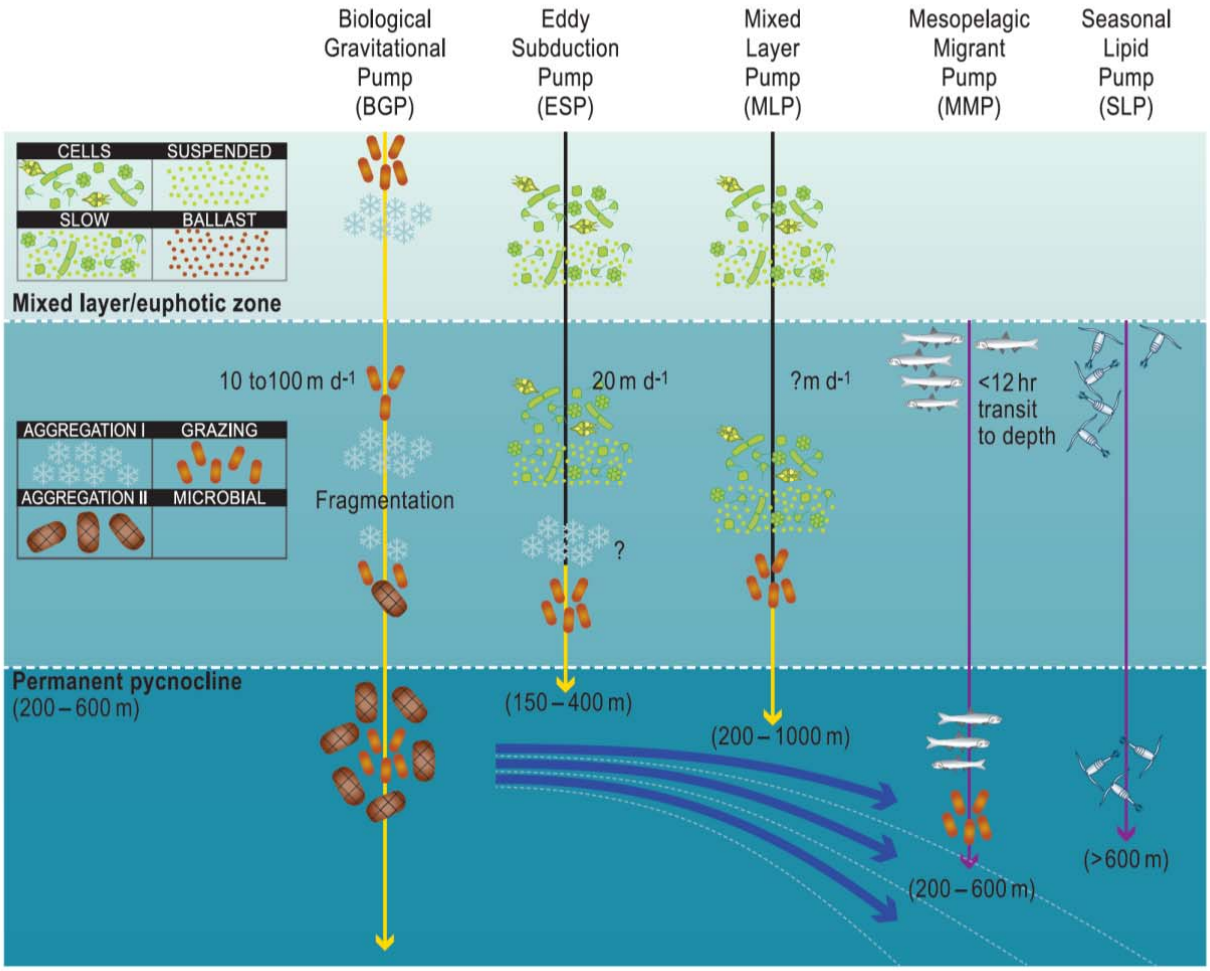

Figure 1 Interplay between particle characteristics, mode of export (BGP or PIP), delivery depth and larger scale ocean circulation for a range of pumps. In the upper panel, the box (top left) represents mixed-layer particle types, which either form large sinking particles (i.e., within the BGP, such as faecal pellets, marine snow) or are injected to depth (i.e., PIPs, suspended/ slow-settling heterogeneous particles and cells (i.e., including healthy, slow-sinking phytoplankton[88])). The vertical yellow arrow signifies the BGP; black lines physically mediated PIPs; and purple lines biologically mediated PIPs. The delivery rates of particles to subsurface strata (in m d^{-1}, ? denotes not known) are presented for each pump. Patchiness in the distribution of vertically-migrating animals (top right) plays a role in driving three-dimensional particle delivery to depth[89,89], and is denoted by different fish or copepod stocks in the upper ocean. The box (middle left) presents different particle transformations central to the BGP[12], but whose role is not known so far for PIPs. They include microbial solubilisation, aggregation (marine snow denoted by aggregation 1; heterogeneous faecally-dominated aggregates (aggregation II) and/or dissaggregation[18] to form/break down heterogeneous particles (hatched brown symbols). In the lower panel, depths in parentheses are the reported delivery depths, with the BGP (and some PIPs) exporting some particles to the sea floor. Blue curved arrows represent transport of subsurface material along downward-sloping isopycnals (white dashed lines). Major unknowns include whether physical transport by PIPs can cause particle aggregation (signified by ? in the middle panel below subduction pump, and also applicable for the mixed-layer pump) and hence alter their mode of injection towards gravitational settling (i.e., the BGP). Other unknowns include the potential ballasting role of small mineral particles such as aerosol dust for PIPs.

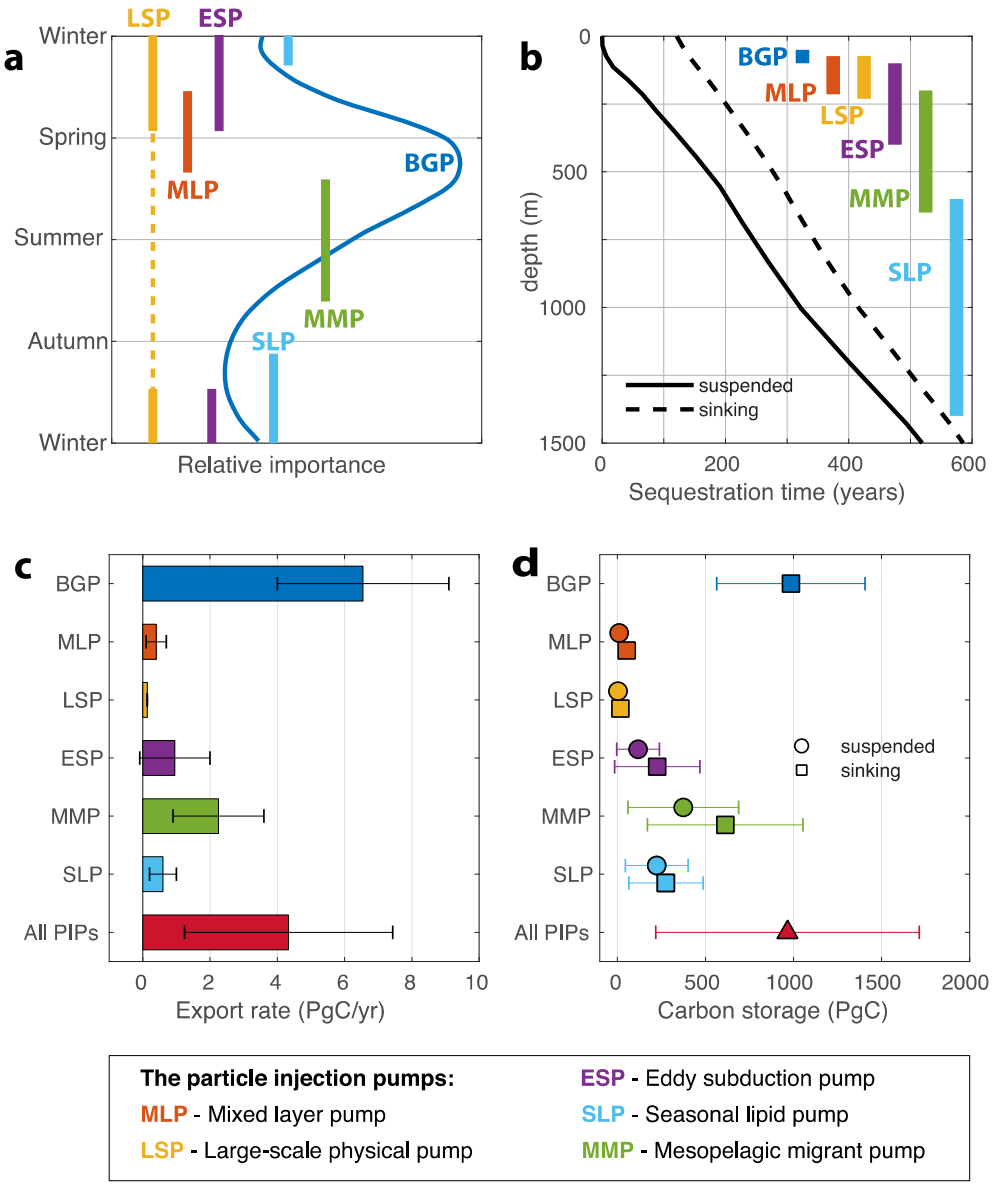

Figure 2 Carbon export and storage by PIPs compared to the BGP. a) Idealised seasonality of the PIPS for regions that exhibit strong seasonality, where a Spring Bloom dominates C export by the BGP (dark blue line). Coloured bars indicate season of peak C export by the PIPs (acronyms defined in legend). Note the large-scale physical pump should be strongest when mixed layers are deepest, but is likely operative all year (dashed line). **b)** Sequestration efficiency of the PIPs. Black lines represent the global-mean sequestration timescale for carbon injected at a given depth, defined as the time for remineralised carbon to circulate back to the ocean surface, computed in a data-constrained circulation model (see S-Methods). Solid line assumes that particles are suspended, so remineralisation occurs at the injection depth, whereas dashed line assumes that particles are sinking and remineralise over depth (see Methods). Colored bars show injection depth range of the BGP and PIPs. The efficiency of each pump is defined as the sequestration time from its injection depth. **c)** Strength of the pump mechanisms, defined as their rate of carbon export or injection (see Table S1). "All PIPs" refers to the sum of the five individual PIPs **d)** Ocean carbon storage by each pump, defined as the product of the strength (**c**) and efficiency (**b**). Two scenarios are shown for each PIP, using the sequestration time for suspended (circles) and sinking (square) particles, whereas the BGP is assumed to export only sinking particles. For the sum of PIPs, we present a "most likely" scenario, in which the migrant pump injects sinking particles (faecal pellets), and all other PIPs inject suspended particles (triangle).

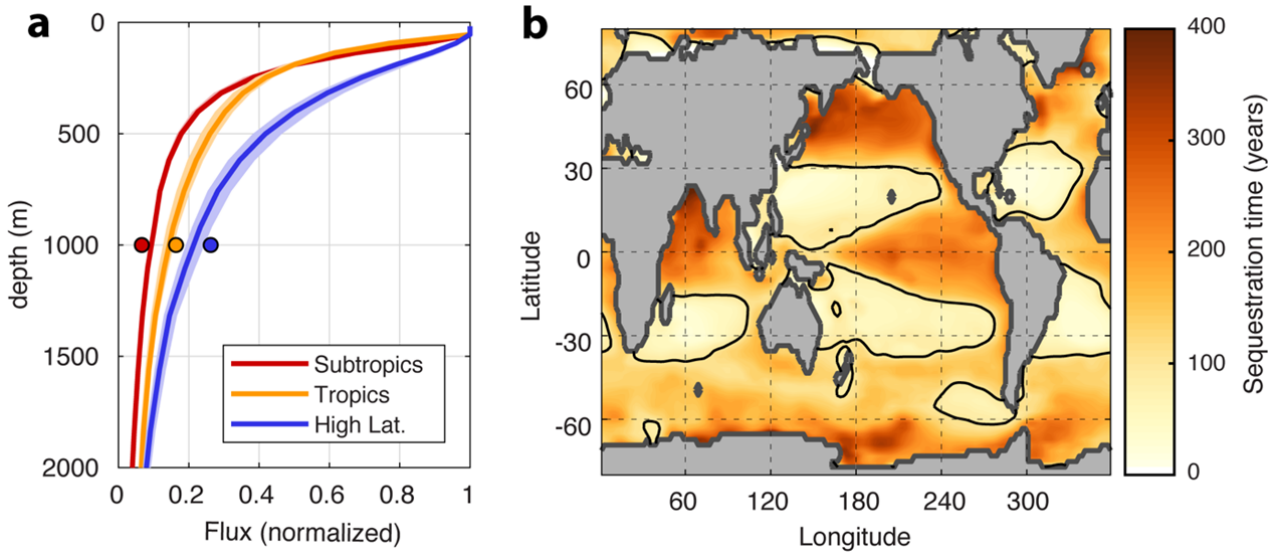

Figure 3. Fate of exported organic matter constrained in models from geochemical remineralisation tracers. a) Organic matter flux over depth (normalised to flux at the base of the euphotic zone), averaged across subtropics, tropics, and high latitude regions (as defined[31]). Lines show flux profiles from a mechanistic model[73] that is optimised to match geochemical constraints (shading represents the range between 12 model configurations); circles represent the transfer efficiency diagnosed directly from nutrient accumulation in an ocean circulation model[31]. **b)** Sequestration time of exported carbon. The spatial pattern reflects both variability in the particle flux attenuation (**a**), and patterns of large-scale circulation. The thin black lines separates regions of efficient (>100 years) and inefficient (<100 years) carbon sequestration.

Box 1 **Approaches used to investigate downward particle export, from the BGP to PIPs.**

The BGP is quantified in a biologically-patchy upper ocean (green filaments) using ship-based surface sampling (particle production) and subsurface particle interception by sediment traps, most recently neutrally-buoyant traps downstream of particle source regions (orange instruments, a). This coupled surface-subsurface sampling strategy is logistically-complex, temporally- and spatially-restricted (i.e., represented here by a "statistical funnel"[91,92], see a), and hence provides a '1D' view of particle export that is extrapolated to the basin scale using satellite observations and/or modelling. This '1D' viewpoint cannot measure the PIPs presented in b) to e), and is contrasted in a) with the 4D view[29,93] obtained by an ensemble of BGC-Argo floats (white instruments).

(b) the mixed-layer pump, in which particles are detrained when the pycnocline (blue dashed line) shallows, can been addressed regionally through backscattering (a proxy for POC) profiles measured by BGC-Argo floats[36], or globally using satellite surface-ocean backscattering and Argo/BGC-Argo (density/backscattering) vertical profiles[32]. c) the seasonal lipid pump is quantified using surveys of overwintering copepods at depths below the permanent pycnocline and subsequent scaling of their lipid-enriched biomass in carbon content[33]. d) the eddy subduction pump can been quantified using gliders (pink instruments) and subsequent modelling[31], BGC-Argo floats (bio-optics/oxygen/physics)[93] or surveys based on multiple POC profiles in conjunction with coupled models (regional circulation/particle dynamics)[30,49]. e) quantification of the mesopelagic migrant pump (active diel transport of carbon by mid-water biota, denoted by moon and sun symbols) requires mid-water trawl surveys along with metabolic modelling[54,55]. Some multidisciplinary studies[30,31,49] have combined these approaches to cross-compare export flux from the BGP (green arrows (d)) and the eddy subduction pump (purple arrows represent subsurface particle maxima recorded at the eddy periphery[31]). Note, the large-scale subduction pump[23] is not presented here.